Anomalous Directed Percolation on a Dynamic Network Using Rydberg Facilitation

Daniel Brady,[1] Simon Ohler,[1] Johannes Otterbach,[2] and Michael Fleischhauer[1]
[1]Department of Physics and Research Center OPTIMAS, RPTU Kaiserslautern, D-67663 Kaiserslautern, Germany
[2]Orthonogal Otter UG, Berlin, Germany

(Received 29 May 2024; revised 15 July 2024; accepted 16 September 2024; published 22 October 2024)

The facilitation of Rydberg excitations in a gas of atoms provides an ideal model system to study epidemic evolution on (dynamic) networks and self-organization of complex systems to the critical point of a nonequilibrium phase transition. Using Monte Carlo simulations and a machine learning algorithm we show that the universality class of this phase transition can be tuned but is robust against decay inherent to the self-organization process. The classes include directed percolation (DP), the most common class in short-range spreading models, and mean-field (MF) behavior, but also different types of anomalous directed percolation (ADP), characterized by rare long-range excitation processes. In a frozen gas, ground state atoms that can facilitate each other form a static network, for which we predict DP universality. With atomic motion the network becomes dynamic by long-range (Lévy-flight type) excitations. This leads to continuously varying critical exponents, varying smoothly between DP and MF values, corresponding to the ADP universality class. These findings also explain the recently observed critical exponent of Rydberg facilitation in an ultracold gas experiment [Helmrich *et al.*, Nature (London) **577**, 481 (2020)], which was in between DP and MF values.

DOI: 10.1103/PhysRevLett.133.173401

Introduction—Nonequilibrium phase transitions [1] and the dynamical self-organization of complex systems to the corresponding critical point [2,3] are key phenomena believed to be the underlying reason for the abundance of scale invariance in nature. They are characteristic for a broad spectrum of spreading processes ranging from epidemic dynamics of diseases [4,5], earthquakes [6], and forest fires [7], to neural networks [8], electric circuits, and information spreading in the internet [9]. The most relevant nonequilibrium phase transitions are those between an active and an inactive phase (absorbing state) of dynamical activity. In contrast to their equilibrium counterpart, they are much less understood. However, the behavior near the critical point shows universal features characterized by different nonequilibrium universality classes [1].

One of the most prominent such universality class is directed percolation (DP) [1], originally describing the flow of fluids through porous materials. Janssen and Grassberger conjectured that nonequilibrium transitions in *any* classical system should belong to the DP universality class if they (i) exhibit a continuous phase transition between an active and a unique absorbing state, (ii) the transition is characterized by a positive one-component order parameter, (iii) the dynamical rules involve only short-range interactions, and (iv) the system has no special attributes such as additional symmetries or quenched randomness [10,11]. To date no counterexamples to these criteria have been found [12], and DP universality has even been predicted in more general systems, e.g., with multiple absorbing states [13,14].

In spite of its the apparent generality only few experimental platforms are known for which DP behavior has unambiguously been proven.

In 2007 the first such platform was found in turbulent liquid crystals and a full set of critical exponents in $d = 2 + 1$ dimensions was measured [15,16]. Since then, interacting systems of Rydberg atoms in the facilitation regime have been suggested to study absorbing state phase transitions, for which DP universal behavior was predicted on a lattice with nearest neighbor interactions [17], and subsequently experimentally observed in a 1D gas [18]. One important aspect, relevant for the emergence of scale invariance, which these model systems lack is the effect of losses from the system. In a *number nonconserving regime* the gas density in the active phase decreases over time which drives the system to its critical point [19,20], a phenomenon called self-organized criticality (SOC) [2,3].

It is not conclusively understood if, and to which extend SOC modifies DP universality [13,19,21]. An experiment investigating Rydberg facilitation in a 3D gas, performed in this number nonconserving regime [19], showed signatures of SOC, but a deviation from DP universality. This deviation was attributed to the self-organization process, as it has been shown that losses can modify the universal properties of the phase transition and may compromise criticality altogether [21]. Specifically in sandpile models dissipation is a relevant perturbation in the renormalization group sense and any degree of bulk dissipation (in the absence of loading) breaks criticality [21,22].

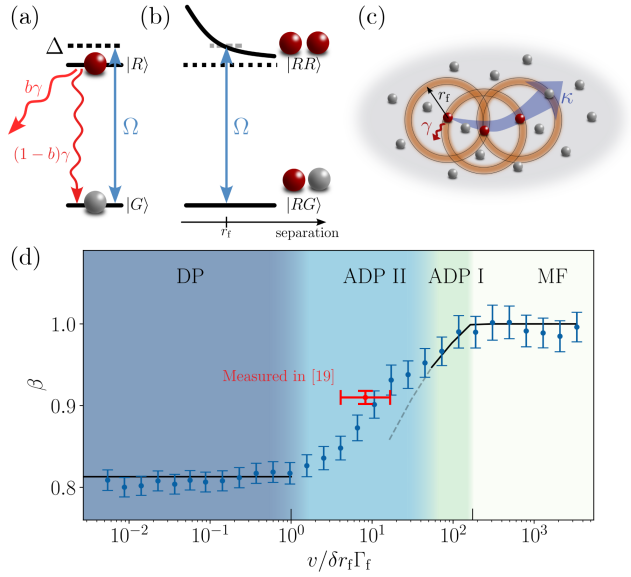

FIG. 1. (a) Single atom dynamics: ground $|G\rangle$ and Rydberg states $|R\rangle$ are laser-coupled with Rabi-frequency Ω and detuning $\Delta \gg \Omega$. $|R\rangle$ decays with rate γ and with branching $b \in [0, 1]$ out of the system. (b) Two atom scheme. Dipole interaction shifts $|RR\rangle$ into resonance at the facilitation distance r_f. (c) Schematic of spreading dynamics: Facilitation is constrained to orange shells with radius r_f and width δr_f. Spreading then occurs at effective rate κ (see main text). (d) Critical exponent β (blue dots, see main text) as a function of mean gas velocity v. Also shown is the theoretical prediction (black line, see main text), for the mean field, directed percolation, and anomalous directed percolation I regimes. Errors in β are given by the covariance matrix when fitting (see text). All points use the parameters $b = 0.3$, $\Delta/\gamma = 2000$, with varied $\Omega/\gamma \in [1, 10]$ and gas density $n_0 r_f^3 \in [20, 30]$.

Through numerical experiments and analytic considerations we show that the deviation in the Rydberg experiment is neither due to SOC [19] nor due to heterogeneity [23], but results from a violation of the Jansen-Grassberger conditions leading to a dependency of the universality class on the relative velocity of the atoms in the gas. Tuning the parameters which set the reference scale of the atomic velocity, the system can either display DP, mean-field (MF), or anomalous directed percolation (ADP) universality. In Fig. 1 numerical results for the critical exponent of the active density around the critical point can be seen as a function of the root mean square (rms) velocity of the atoms. Also shown is the critical exponent measured in [19] along with the estimated region of velocities in the experiment ranging between the average thermal velocity of the atoms and that resulting from the acceleration in the repulsive Van der Waals potential.

Several real-life spreading processes go beyond the Janssen-Grassberger conjecture. For example, the spread of diseases by flying insects in addition to direct contact violates the condition of short-range excitations [24,25]. Likewise, spreading processes often take place on dynamical rather than static networks [26]. These often change on a timescale comparable with that of the spreading process [27].

Microscopic system—We consider a three-dimensional gas of N atoms coupled between a ground $|G\rangle$ and a Rydberg $|R\rangle$ state with a laser with Rabi frequency Ω and detuning Δ [see Fig. 1(a)]. The unitary dynamics are described by the Hamiltonian $\hat{H} = \sum_i \Omega\hat{\sigma}_i^x - \Delta\hat{\sigma}_i^{rr} + \sum_{j<i}(c_6/r_{ij}^6)\hat{\sigma}_i^{rr}\hat{\sigma}_j^{rr}$, where $\hat{\sigma}_i^{rr}$ is the projection operator of the ith atom onto its Rydberg state, c_6 is the Van der Waals coefficient for the Rydberg-Rydberg interaction potential, and $r_{ij} = |\vec{r}_i - \vec{r}_j|$ is the distance between atoms i and j.

In addition to the unitary dynamics, we account for spontaneous decay of the Rydberg state into the ground or an additional dark state $|0\rangle$ described by the jump operators $\hat{L}_{1,i} = \sqrt{(1-b)\gamma}|G\rangle_{ii}\langle R|$ and $\hat{L}_{2,i} = \sqrt{b\gamma}|0\rangle_{ii}\langle R|$, respectively. Here the parameter $b \in [0, 1]$ describes the portion of atoms lost from the system, e.g., following decay into inert states, or state-changing collisions. Finally, dephasing is accounted for by $\hat{L}_{3,i} = \sqrt{\gamma_\perp}|R\rangle_{ii}\langle R|$. Typically in Rydberg gases $\gamma_\perp \geq \Omega$, allowing classical rate equations to describe these systems to high accuracy [28].

The evolution of the N-body density matrix is given by the Lindblad master equation $(\mathrm{d}/\mathrm{d}t)\hat{\rho} = -i[\hat{H}, \hat{\rho}] + \hat{\mathcal{L}}(\hat{\rho})$, with the superoperator $\hat{\mathcal{L}}(\hat{\rho})$ [29]. After adiabatic elimination of coherences a set of rate equations for the occupation probabilities in Rydberg (p_r^j) and ground states (p_g^j) of the jth atom can be derived. These read

$$\frac{\mathrm{d}}{\mathrm{d}t}p_r^j = -(\Gamma_j + \gamma)p_r^j + \Gamma_j p_g^j, \quad \frac{\mathrm{d}}{\mathrm{d}t}(p_r^j + p_g^j) = -b\gamma p_r^j, \qquad (1)$$

where the rate $\Gamma_j = 2\Omega^2\gamma_\perp/(\gamma_\perp^2 + V_j^2)$ with $V_j = \Delta[-1 + \sum_{l\in\Sigma}(r_f^6/r_{jl}^6)]$ depends on the dipole-dipole shift induced by all other Rydberg atoms denoted by Σ.

For all simulations we initiate random positions in a 3D box with length $L = 7r_f$ and periodic boundary conditions. Atom velocities are sampled from a Maxwell-Boltzmann distribution, i.e., a Gaussian in each direction, with rms velocity v. Furthermore, we use $\gamma_\perp/\gamma = 20$ and a Monte Carlo algorithm [30] with fixed time step $\gamma dt = 0.0025$.

For Rydberg facilitation systems, atoms are continuously driven far from resonance, i.e., $\Delta \gg \Omega$. As a result of the strong detuning, off-resonant (seed) excitations are strongly suppressed. However, in the presence of a Rydberg atom, other atoms with distance $r \approx r_f \equiv \sqrt[6]{(C_6/\Delta)}$ are shifted into resonance as a result of the vdW interaction [see Fig. 1(b)].

Consequently, atoms within a spherical shell with volume $V_s \approx 4\pi\delta r_f r_f^2$ around a Rydberg atom can be *facilitated* (i.e., excited on much faster timescales). Here $\delta r_f \approx (\gamma_\perp/2\Delta)r_f$ is the width of the facilitation shell. The rate of excitation for atoms within the facilitation shell is

$\Gamma_f = 2\Omega^2/\gamma_\perp$. Facilitation can also be interpreted as infection processes, with a global spreading rate $\kappa = \Gamma_f n V_s$, where n is the gas density. Spontaneous decay of Rydberg atoms back to the ground state then corresponds to recovery with rate γ.

Critical scaling—These systems feature a nonequilibrium phase transition between an absorbing phase, for $\kappa < \gamma$, with no excited atoms in the thermodynamic limit, and an active phase, for $\kappa > \gamma$, featuring widespread and infinitely long-lived activity. Near the critical driving strength $\kappa \approx \gamma$, there is universal behavior characterized by scaling relations for the Rydberg density ρ, as well as the temporal and spatial correlation lengths, $\xi_\parallel$ and $\xi_\perp$, respectively,

$$\rho \sim (p - p_c)^\beta, \qquad \xi_{\parallel,\perp} \sim |p - p_c|^{-\nu_{\parallel,\perp}}. \tag{2}$$

Here $p - p_c$ corresponds to the distance of the control parameter from the critical point, and β, $\nu_\parallel$, $\nu_\perp$ are critical exponents. Finally, while seed excitations are strongly suppressed, they still occur with rate $\tau \sim 1/\Delta^2$.

In the following, we consider the system in the SOC regime, allowing Rydberg atoms to additionally decay to an inert state, effectively removing them from the system, with the rate $b\gamma$ [see Fig. 1(a)]. As a consequence, the system drives itself to the critical density given in MF approximation by $n_c = (\Delta\gamma/4\pi\Omega^2) r_f^{-3}$.

The SOC dynamics for different initial gas densities can be seen in Fig. 2(a). In the initial active phase there is a fast loss of atoms to inert states until the critical point is reached where this loss slows down substantially. To observe universal critical behavior these two timescales must be well separated [31].

Since an infinite separation of timescales is not numerically feasible, a slow decay of the density at the critical point is expected [this can be seen in Fig. 2(a)]. This, however, poses a challenge for the determination of the critical density. To this end, we trained a machine learning (ML) algorithm to predict n_c based on the time-dependent density $n(t)$ [32]. Predictions of n_c can be seen in Fig. 2(a) as horizontal dashed lines for each trajectory.

For the critical scaling we first consider the limit where the thermal movement of atoms occurs on a much slower timescale than the internal dynamics, rendering them effectively static (i.e., the thermal gas velocity is $v < \delta r_f \Gamma_f$.) In this *frozen-gas* limit, the spreading of excitations is constrained to a random Erdős-Rényi network with the average network degree $\langle k \rangle$ given by $\langle k \rangle = n V_s$ [34].

At $\langle k \rangle = 1$ a transition occurs between a nonpercolating network of ground state atoms with distance r_f, composed of many small disconnected clusters, and a percolating network with one large cluster on the order of the size of the system [35]. For $\langle k \rangle < 1$ this gives rise to a heterogeneous, nonuniversal Griffiths phase replacing the critical point. Above the percolation transition, however, i.e., $\langle k \rangle > 1$, the absorbing-state phase transition is recovered [34,36]. (The SOC dynamics do not change the Erdős-Rényi character of the network, but only lead to a reduction of $\langle k \rangle$).

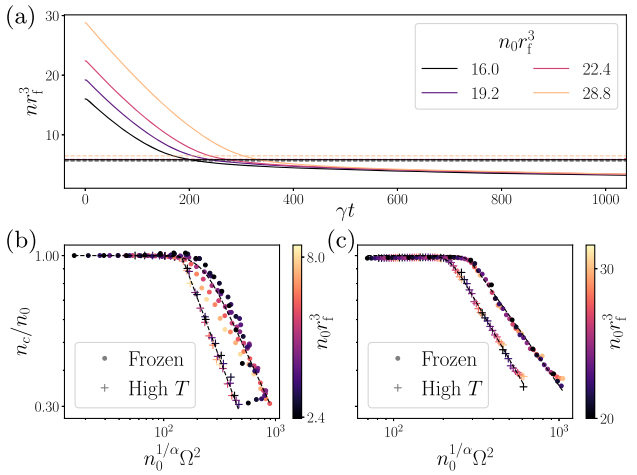

FIG. 2. (a) SOC dynamics of density of ground and Rydberg atoms in high temperature limit ($v/\delta r_f \Gamma_f = 5443$) for $b = 0.3$, $\Omega/\gamma = 3.7$, and $\Delta/\gamma = 1000$, with varied n_0 showing self-organized criticality to a single density n_c. Machine learning predictions of the critical density for each trajectory (horizontal dashed lines) and n_c (horizontal solid black line). (b) ML predictions of critical density n_c normalized by initial density n_0 depending on the rescaled driving (see main text) for (b) the nonpercolating gas, $\langle k \rangle < 1$ (left) and (c) for the percolating gas, $\langle k \rangle > 1$ (right) for both frozen ($v/\delta r_f \Gamma_f = 0$) and high temperature ($v/\delta r_f \Gamma_f = 5443$) limits. The exponent α is tuned until all data points collapse. For the frozen, nonpercolating gas no collapse can be found.

At high gas temperatures the continuous mixing of atomic positions and subsequent fast decay of spatial correlations leads to mean field behavior regardless of $\langle k \rangle$ [37].

An unambiguous signature of universal behavior and a precise method for the classification into a certain universality class is the collapse of data obtained over a large parameter range onto specific scaling functions. Following Ref. [19], we consider the density of atoms in active states (i.e., in the ground and Rydberg state, but not in the inert state) at the critical point n_c, normalized to the initial density n_0 as a function of the generalized driving strength $\Omega^2 n_0^{1/\alpha}$, with α being tuned until all data points collapse onto a single curve. Scale invariance requires

$$\frac{n_c}{n_0} = f\left(\Omega^2 n_0^{1/\alpha}\right) \tag{3}$$

to hold over the entire parameter range, with a scaling function $f(x)$, which can be chosen as $f(x) = x_c^\beta (x^{\mu\beta} + x_c^{\mu\beta})^{-1/\mu}$ [19], where x_c and μ are free parameters defining the position and sharpness of the critical point. Finally, β corresponds to the critical exponent from Eq. (2).

For both high temperature and frozen limits, the results are plotted in Figs. 2(b) and 2(c) for $\langle k\rangle < 1$ and $\langle k\rangle > 1$, respectively. For the high temperature limit we receive a collapse of all data points onto a single power-law using $\alpha = 1.08(1)$ ($\langle k\rangle < 1$) and $\alpha = 1.26(1)$ ($\langle k\rangle > 1$). We then extract the critical exponents $\beta_{\mathrm{low}}\langle k\rangle = 1.049(19)$ and $\beta_{\mathrm{high}}\langle k\rangle = 0.996(18)$, respectively, which both fall in line with the expected mean field exponent $\beta_{\mathrm{MF}} = 1.00$. Errors are calculated from the covariance matrix of the fit parameters.

For the low temperature regime, on the other hand, [dots in Figs. 2(b) and 2(c)] we find no collapse of data below the percolation threshold, i.e., $\langle k\rangle < 1$, for values of $\alpha \in [0.5, 2.0]$, indicating nonuniversal behavior which is consistent with a heterogeneous Griffiths phase [34]. For $\langle k\rangle > 1$, however, the data collapse onto a single power-law for $\alpha = 0.88(1)$, with the slope clearly differing from the high temperature one. Furthermore, when using the above mentioned fit function we obtain the power-law exponent $\beta_{\mathrm{frozen}} = 0.809(13)$, very close to the expected 3D DP critical exponent $\beta_{\mathrm{DP}} \approx 0.813$ [12].

To unambiguously confirm DP and MF universality in the low and high temperature limits, we also determine the critical exponent $\nu_{\parallel}$ governing temporal correlations around the critical point. We find a good agreement with literature values. A detailed analysis including numerical results can be found in Supplemental Material [32].

Anomalous directed percolation—From the above discussion one would naively expect that there is a critical value of the mean gas velocity where a phase transition between DP and MF behavior takes place. Astonishingly however, we find for gas temperatures between the two limits (and $\langle k\rangle > 1$) a universal collapse of data points with a *monotonously changing critical exponent* β over multiple orders of magnitude in the rms gas velocity [Fig. 1(d)].

Increasing the temperature the system leaves the DP regime at rather low velocities corresponding to the (very small) width of the facilitation shell per facilitation time, i.e., $v_- = \delta r_{\mathrm{f}}\Gamma_{\mathrm{f}}$ (left mark in Fig. 1). This is due to the number of ground-state atoms that can be facilitated by a single Rydberg atom increasing once this velocity is exceeded. On the other hand, for velocities greater than $v_+ = r_{\mathrm{f}}\Gamma_{\mathrm{f}}$, i.e., when an atom flies distances larger than the facilitation distance in the facilitation time, the network character of (ground) state atoms becomes completely washed out (right mark in Fig. 1).

In the following we show that the critical behavior with continuously varying β in the velocity range between these two limiting values is a signature of ADP universality, resulting from effective long-range spreading processes and heavy-tailed waiting time distributions [38].

Absorbing-state phase transitions in complex systems where excitation distances follow a Lévy flight distribution for large r as

$$P(r) \sim \frac{1}{r^{d+\sigma}}, \tag{4}$$

where d is the dimension and σ is a free parameter, no longer fulfill the Janssen-Grassberger conjecture if σ becomes too small. Such systems, however, still show universal behavior, albeit with continuously varying critical exponents depending on the value of σ [12,38]. The same is true if the distribution of time intervals between successive excitations [i.e., waiting time distribution $P(\delta t)$] is heavy tailed. In general, the algebraic spatial and temporal distributions effectively reduce the upper critical dimension, and the critical exponents approach the MF values.

In the frozen gas limit each atom is confined to a cluster and has k atoms in its facilitation shell, with k given by a Poissonian distribution as $P(k) = [(nV_s)^k/k!]\mathrm{e}^{-nV_s}$. With increasing thermal velocity, the probability that an atom finds another connection outside of its original cluster increases. Since the underlying network is a random network, even small distances in real space can correspond to completely new connections, i.e., very distant jumps in the network.

For an initially excited Rydberg atom with velocity v, the distribution of distances to the next facilitated atom can be seen in Fig. 3(a), where the dots are from MC simulations. Outside of the facilitation shell (vertical black dashed line), we find that this probability decays as a power-law with an exponent σ decreasing with increasing atom velocity. For large distances around v/Γ_{f} the excitation probability is exponentially truncated.

This distribution can be described analytically outside of the facilitation shell by

$$P(r) = 2\pi\xi r \int_0^{\pi} \mathrm{d}\theta \frac{\mathrm{e}^{-\xi\left(\sqrt{\cos^2\theta + r^2 - 1} - \cos\theta\right)}}{\sqrt{\cos^2\theta + r^2 - 1}}, \tag{5}$$

with $\xi = (\langle k\rangle/\delta r_{\mathrm{f}})(1 - \mathrm{e}^{-\delta r_{\mathrm{f}}\Gamma_{\mathrm{f}}/v})$ [black solid line in Fig. 3(a)]. The derivation of Eq. (5) can be found in the Supplemental Material [32].

In 3D systems, (long-range) MF behavior occurs for $\sigma < 1.5$ [lower black dashed line in Fig. 3(b)], while for $\sigma > 2.118(17)$ regular DP behavior is expected [upper black dashed line in Fig. 3(b)] [12]. In between these limits, the long range interactions are prevalent enough to disrupt DP universality, but not strong enough to suppress all correlations. Here, the system is governed by a family of continuously varying universality classes (ADP), labeled by the long-range parameter σ [12].

Fitting the spatial distribution of excitation distances with an exponentially truncated power-law $f(x) = c_1 x^{-c_2}\mathrm{e}^{-c_3 x}$, with $c_2 = \sigma - 1$ [as $P(\vec{r})\mathrm{d}^3x = P(r)4\pi r^2\mathrm{d}r$], we receive very good agreement between the data and the fit function [dashed lines in Fig. 3(a)]. From this we can extract the power-law slope $\sigma(v)$ governing the flight

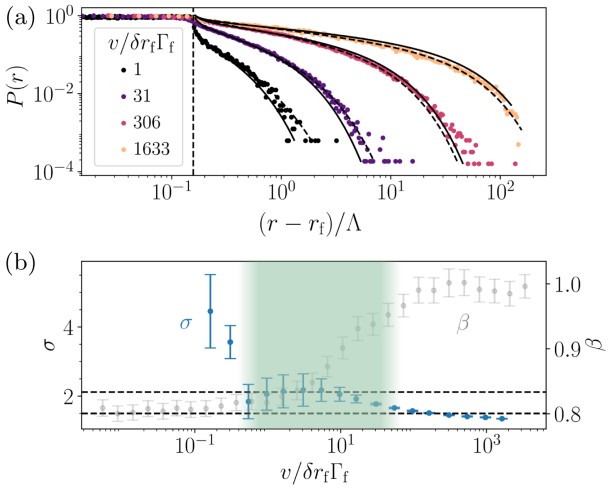

FIG. 3. (a) Distribution of distances between excitations in units of mean free path Λ for different rms gas velocities v. Half width of facilitation shell is given by vertical gray dashed line. The black dashed lines are combined power-law and exponential fits and the black solid lines are analytical predictions given by Eq. (5). (b) Power-law exponent σ (blue) of excitation distance distribution [from fit in (a)] and field theoretical limits of ADP (horizontal dashed lines), as well as critical scaling exponent β (gray) continuously changing between MF and DP plateaus for gas velocities where σ is within ADP bounds. In the green shaded region the distribution of times between excitations deviates from exponential. Both plots use $\Omega/\gamma = 20$, $\Delta/\gamma = 2000$, $n_0 r_f^3 = 20$.

distance distribution depending on the thermal gas velocity seen in Fig. 3(b).

For the distribution of times between excitations (see Supplemental Material [32]), we find a deviation from a pure exponential distribution for gas velocities in the interval $v/\delta r_f\Gamma_f \in [0.5, 50.0]$. In this regime [reflected by the green shaded region in Fig. 3(b)], spatial and temporal long-range processes are relevant.

For gas velocities in the interval $v/\delta r_f\Gamma_f \in [50, 160]$, we find an exponential waiting time distribution, but a spatial power-law distribution with $\sigma > 1.5$, giving rise to the ADP I regime [1]. Here the critical exponents β and $\nu_\parallel$ can be field theoretically approximated in perturbation theory to one-loop order, which yields [12] for $\sigma > 1.5$

$$\beta = 1 - 2\frac{2\sigma - 3}{7\sigma}, \qquad \nu_\parallel = 1 + \frac{2\sigma - 3}{7\sigma^2}, \tag{6}$$

and $\beta = \nu_\parallel = 1$ for $\sigma \leq 1.5$. For gas velocities $v/\delta r_f\Gamma_f \gtrsim 50$ we see a very good agreement between the field theoretical approximation of $\beta[\sigma(v)]$ and our simulation results (black line in Fig. 1). With decreasing velocity, i.e., entering the ADP II regime, the field theoretical predictions begin to diverge (gray dashed line in Fig. 1) resulting from the nonexponential distribution in waiting times and the failure of the perturbation expansion.

Conclusion—Systems of facilitated Rydberg excitations form an accessible experimental platform to investigate nonequilibrium dynamics. Using Monte Carlo simulations we discover the existence of rare Lévy-flight type excitations which, if prevalent enough, can alter the universality class of the nonequilibrium phase transition in the system. This deviation from directed percolation universality was previously assumed to be a result of self-organized criticality. However, for low temperatures we find critical exponents which coincide with DP universality while the system also displays SOC.

One important aspect is whether all universality classes can be experimentally realized. For typical ultracold Rydberg gases temperatures below 1 μK [39] are reachable. The critical temperature to reach the DP regime is given by $v_- = \delta r_f\Gamma_f \equiv (\kappa/4\pi r_f^2)$ (explicitly $T_- = (m\kappa/3k_B 4\pi r_f^2)$, with the atom mass m). For the parameters used in [19] this becomes $T_- \approx 7$ μK.

Acknowledgments—Financial support from the DFG through SFB TR 185, Project No. 277625399, is gratefully acknowledged. The authors also thank the Allianz für Hochleistungsrechnen (AHRP) for giving us access to the "Elwetritsch" HPC Cluster.

[1] H. Hinrichsen, Non-equilibrium critical phenomena and phase transitions into absorbing states, Adv. Phys. **49**, 815 (2000).
[2] P. Bak, C. Tang, and K. Wiesenfeld, Self-organized criticality, Phys. Rev. A **38**, 364 (1988).
[3] P. Bak, *How Nature Works: The Science of Self-Organized Criticality* (Springer Science & Business Media, New York, 2013).
[4] N. T. Bailey *et al.*, *The Mathematical Theory of Infectious Diseases and its Applications* (Charles Griffin & Company Ltd., Bucks, 1975).
[5] R. Pastor-Satorras, C. Castellano, P. Van Mieghem, and A. Vespignani, Epidemic processes in complex networks, Rev. Mod. Phys. **87**, 925 (2015).
[6] A. Sornette and D. Sornette, Self-organized criticality and earthquakes, Europhys. Lett. **9**, 197 (1989).
[7] B. Drossel and F. Schwabl, Self-organized critical forest-fire model, Phys. Rev. Lett. **69**, 1629 (1992).
[8] N. Friedman, S. Ito, B. A. W. Brinkman, M. Shimono, R. E. Lee DeVille, K. A. Dahmen, J. M. Beggs, and T. C. Butler, Universal critical dynamics in high resolution neuronal avalanche data, Phys. Rev. Lett. **108**, 208102 (2012).
[9] L. A. Adamic and B. A. Huberman, Power-law distribution of the world wide web, Science **287**, 2115 (2000).
[10] H.-K. Janssen, On the nonequilibrium phase transition in reaction-diffusion systems with an absorbing stationary state, Z. Phys. B Condens. Matter **42**, 151 (1981).
[11] P. Grassberger, On phase transitions in Schlögl's second model, Z. Phys. B Condens. Matter **47**, 365 (1982).
[12] H. Hinrichsen, Non-equilibrium phase transitions, Physica (Amsterdam) **369A**, 1 (2006).

[13] M. A. Muñoz, G. Grinstein, R. Dickman, and R. Livi, Critical behavior of systems with many absorbing states, Phys. Rev. Lett. **76**, 451 (1996).
[14] M. Muñoz, G. Grinstein, and R. Dickman, Phase structure of systems with infinite numbers of absorbing states, J. Stat. Phys. **91**, 541 (1998).
[15] K. A. Takeuchi, M. Kuroda, H. Chaté, and M. Sano, Directed percolation criticality in turbulent liquid crystals, Phys. Rev. Lett. **99**, 234503 (2007).
[16] K. A. Takeuchi, M. Kuroda, H. Chaté, and M. Sano, Experimental realization of directed percolation criticality in turbulent liquid crystals, Phys. Rev. E **80**, 051116 (2009).
[17] M. Marcuzzi, E. Levi, W. Li, J. P. Garrahan, B. Olmos, and I. Lesanovsky, Non-equilibrium universality in the dynamics of dissipative cold atomic gases, New J. Phys. **17**, 072003 (2015).
[18] R. Gutiérrez, C. Simonelli, M. Archimi, F. Castellucci, E. Arimondo, D. Ciampini, M. Marcuzzi, I. Lesanovsky, and O. Morsch, Experimental signatures of an absorbing-state phase transition in an open driven many-body quantum system, Phys. Rev. A **96**, 041602(R) (2017).
[19] S. Helmrich, A. Arias, G. Lochead, T. Wintermantel, M. Buchhold, S. Diehl, and S. Whitlock, Signatures of self-organized criticality in an ultracold atomic gas, Nature (London) **577**, 481 (2020).
[20] D.-S. Ding, H. Busche, B.-S. Shi, G.-C. Guo, and C. S. Adams, Phase diagram and self-organizing dynamics in a thermal ensemble of strongly interacting Rydberg atoms, Phys. Rev. X **10**, 021023 (2020).
[21] J. A. Bonachela and M. A. Muñoz, Self-organization without conservation: True or just apparent scale-invariance?, J. Stat. Mech. (2009) P09009.
[22] K. B. Lauritsen, S. Zapperi, and H. E. Stanley, Self-organized branching processes: Avalanche models with dissipation, Phys. Rev. E **54**, 2483 (1996).
[23] T. M. Wintermantel, M. Buchhold, S. Shevate, M. Morgado, Y. Wang, G. Lochead, S. Diehl, and S. Whitlock, Epidemic growth and Griffiths effects on an emergent network of excited atoms, Nat. Commun. **12**, 103 (2021).
[24] D. Mollison, Spatial contact models for ecological and epidemic spread, J. R. Stat. Soc. Ser. B **39**, 283 (1977).
[25] P. Grassberger, *Fractals in Physics*, edited by L. Pietronero and E. Tosatti (Elsevier, New York, 2012).
[26] P. Holme and J. Saramäki, Temporal networks, Phys. Rep. **519**, 97 (2012).
[27] K. Zhao, M. Karsai, and G. Bianconi, Entropy of dynamical social networks, PLoS One **6**, e28116 (2011).
[28] E. Levi, R. Gutiérrez, and I. Lesanovsky, Quantum non-equilibrium dynamics of Rydberg gases in the presence of dephasing noise of different strengths, J. Phys. B **49**, 184003 (2016).
[29] G. Lindblad, On the generators of quantum dynamical semigroups, Commun. Math. Phys. **48**, 119 (1976).
[30] V. R. Barlett, J. Bigeón, M. Hoyuelos, and H. Mártin, Differences between fixed time step and kinetic Monte Carlo methods for biased diffusion, J. Comput. Phys. **228**, 5740 (2009).
[31] D. Marković and C. Gros, Power laws and self-organized criticality in theory and nature, Phys. Rep. **536**, 41 (2014).
[32] See Supplemental Material at http://link.aps.org/supplemental/10.1103/PhysRevLett.133.173401, which includes Ref. [33] for a description of the machine learning algorithm, a derivation of Eq. (5), as well as a discussion on further distributions and critical exponents.
[33] P. J. Huber, Robust estimation of a location parameter, Ann. Math. Stat. **35**, 73 (1964).
[34] D. Brady, J. Bender, P. Mischke, S. Ohler, T. Niederprüm, H. Ott, and M. Fleischhauer, Griffiths phase in a facilitated Rydberg gas at low temperatures, Phys. Rev. Res. **6**, 013052 (2024).
[35] P. Erdős and A. Rényi, On the evolution of random graphs, Publ. Math. Inst. Hung. Acad. Sci **5**, 17 (1960).
[36] M. A. Muñoz, R. Juhász, C. Castellano, and G. Ódor, Griffiths phases on complex networks, Phys. Rev. Lett. **105**, 128701 (2010).
[37] D. Brady and M. Fleischhauer, Mean-field approach to Rydberg facilitation in a gas of atoms at high and low temperatures, Phys. Rev. A **108**, 052812 (2023).
[38] H. Hinrichsen, Non-equilibrium phase transitions with long-range interactions, J. Stat. Mech. (2007) P07006.
[39] A. D. Bounds, N. C. Jackson, R. K. Hanley, R. Faoro, E. M. Bridge, P. Huillery, and M. P. A. Jones, Rydberg-dressed magneto-optical trap, Phys. Rev. Lett. **120**, 183401 (2018).